

KINEMATIC AGES OF CENTRAL STARS OF PLANETARY NEBULAE

W. J. Maciel,¹ T. S. Rodrigues¹ and R. D. D. Costa,¹

Draft version: October 19, 2018

RESUMEN

ABSTRACT

The age distribution of the central stars of planetary nebulae (CSPN) is estimated using two methods based on their kinematic properties. First, the expected rotation velocities of the nebulae at their Galactocentric distances are compared with the predicted values for the rotation curve, and the differences are attributed to the different ages of the evolved stars. Adopting the relation between the ages and the velocity dispersions determined by the Geneva-Copenhagen survey, the age distribution can be derived. Second, the U, V, W, velocity components of the stars are determined, and the corresponding age-velocity dispersion relations are used to infer the age distribution. These methods have been applied to two samples of PN in the Galaxy. The results are similar for both samples, and show that the age distribution of the PN central stars concentrates in ages lower than 5 Gyr, peaking at about 1 to 3 Gyr.

Key Words: ISM: planetary nebulae: general — Stars: AGB and Post-AGB — Stars: general — Stars: fundamental parameters

1. INTRODUCTION

Planetary nebulae (PN) are evolved objects ejected by stars with main sequence masses in the range of 0.8 and 8 M_{\odot} , so that the expected ages of their central stars are of the order or greater than about 1 Gyr. However, the relatively large mass bracket of their progenitor stars implies that an age distribution is to be expected, which has some consequences in the interpretation of the PN data in the Galaxy and other stellar systems. The determination of ages of the central stars is a difficult problem, and most usual methods have large uncertainties when applied to intermediate and old age objects. We have recently developed three different methods to estimate the age distribution of the CSPN (Maciel, Costa & Idiart 2010, see also Maciel et al. 2003, 2005, 2006), and applied these methods to a sample of PN in the disk of the Galaxy, most of which are located in the solar neighbourhood, within 3 kpc from the Sun. These methods include the determination of the age distribution of CSPN using (i) an age-metallicity relation that also depends on the Galactocentric distance, (ii) an age-metallicity relation obtained for

¹Instituto de Astronomia, Geofísica e Ciências Atmosféricas, Universidade de São Paulo, Brazil.

the disk, and (iii) the central star masses obtained from the observed nitrogen abundances. We concluded that most CSPN in our sample have ages under 6 Gyr, and that the age distribution is peaked around 2-4 Gyr. The average uncertainties were estimated as 1-2 Gyr, and the results were compared with the expected distribution based both on the observed mass distribution of white dwarfs and on the age distribution derived from available masses of CSPN.

In the present work we develop two additional and more accurate methods to estimate the age distribution of the CSPN based on their kinematical properties, namely: (i) A method based on the expected rotation velocities of the nebulae at their Galactocentric distances, which are then compared with the predicted values for a given rotation curve; the differences are attributed to the different ages of the evolved stars; (ii) A method based on the derived U, V, W, velocity components of the stars and their corresponding dispersions. In both cases, the age-velocity dispersion relations from the Geneva-Copenhagen survey are used to infer the age distribution. These methods are applied to two PN samples, (i) the previous sample of disk PN used by Maciel, Costa & Idiart (2010), for which a detailed data set is available, and (ii) a sample containing all PN for which accurate radial velocities are known. The methods are developed in Section 2, and the samples used are described in Section 3. The main results and discussion are given in Section 4.

2. DETERMINATION OF THE AGE DISTRIBUTION OF CSPN

2.1. Method 1: The PN rotation velocity

As objects of intermediate age, PN the disk of the Galaxy describe a rotation curve similar to the one defined by younger objects, such as HII regions, although with a higher dispersion, as discussed in detail by Maciel and Lago (2005). Therefore, the discrepancies between the rotation velocities inferred from the PN radial velocities and distances and the expected velocities from the known rotation curve may be at least partially ascribed to their evolved status. In other words, a given nebulae located at a distance d , with galactic coordinates ℓ and b and observed heliocentric radial velocity $V_r(hel)$ can be associated with a rotation velocity $\theta(R)$, after obtaining its Galactocentric distance R and its radial velocity relative to the Local Standard of Rest (LSR), $V_r(LSR)$. Assuming circular orbits, the rotation velocity $\theta(R)$ at the Galactocentric distance R can be written as

$$\theta(R) = \frac{R}{R_o} \left[\frac{V_r(LSR)}{\sin \ell \cos b} + \theta_0 \right] \quad (1)$$

where R_o and θ_0 are the Galactocentric distance and rotation velocity at the solar position (see for example Maciel & Lago 2005, Maciel & Dutra 1992). On the other hand, the expected rotation velocity at the given Galactocentric distance, $\theta_c(R)$, can be obtained from an adopted rotation curve. The difference $\Delta\theta = |\theta(R) - \theta_c(R)|$ can then be considered as proportional to the age

TABLE 1
COEFFICIENTS OF THE POLYNOMIAL GIVEN BY EQ. (3).

R (kpc)	0 – 0.765	0.765 – 2.9	2.9 – 3.825	3.825 – 13	> 13
a_0	0.0	325.0912	329.8	–2346.0	230.6
a_1	3069.81	–248.1467	–250.1	2507.60391	–
a_2	–15809.8	231.87099	231.87099	–1024.068760	–
a_3	43980.1	–110.73531	–110.73531	224.562732	–
a_4	–68287.3	25.073006	25.073006	–28.4080026	–
a_5	54904.0	–2.110625	–2.110625	2.0697271	–
a_6	–17731.0	–	–	–0.080508084	–
a_7	–	–	–	0.00129348	–

difference between the PN and the objects defining the rotation curve. We have adopted the radial velocities from the catalogue by Durand et al. (1998), and two distance scales, those by Maciel (1984) and Stanghellini et al. (2008). The first one was based on a relationship between the ionized mass and the radius of the nebulae, while the second is an update of the distance scale by Cahn et al. (1992), using a modified Shklovsky method following Daub (1982). Since the distances of planetary nebulae in the Galaxy may contain large individual uncertainties, the use of two different scales which are considered as “short” (Maciel 1984) and “long” (Stanghellini et al. 2008) warrants that these uncertainties will not affect the derived age distributions. We have adopted $R_0 = 8.0$ kpc for the distance of the Sun to the centre and $\theta_0 = 220$ km/s for the rotation velocity at R_0 . Slightly different values can be found in the literature (see for example Perryman, 2009, and Reid, 2010), but the values above are frequently adopted, so that a comparison with other works is made easier. For the “theoretical” rotation curve we have also adopted two possibilities, namely, the PN derived curve by Maciel & Lago (2005), and the HII region derived curve by Clemens (1985). In the first case, the rotation velocity can be written as

$$\theta_c(R) = a_0 + a_1 R + a_2 R^2 . \quad (2)$$

where the constants are $a_0 = 269.2549$, $a_1 = -14.7321$, and $a_2 = 0.7847$, the Galactocentric distance R is in kpc and $\theta_c(R)$ in km/s. For the CO/HII region based Clemens (1985) curve, we have made an adjustment for $R_0 = 8.0$ kpc and $\theta_0(R) = 220$ km/s, in which case we have

$$\theta_c(R) = \sum a_i R^i . \quad (3)$$

where the constants are given in Table 1, with the same units as in Eq.(2).

TABLE 2
COEFFICIENTS OF EQ. (4).

	a	b
U	0.39	1.31
V	0.40	1.10
W	0.53	0.94
Total	0.40	1.40

The recent Geneva-Copenhagen Survey of the Solar Neighbourhood (cf. Nordström et al. 2004, Holmberg et al. 2007, 2009) has considerably improved the relations involving the ages, kinematics, and chemical composition of a large sample containing about 14000 F and G nearby stars. Using basically the original *Hipparcos* parallaxes, *uvby β* photometry and the Padova stellar evolution models, several basic relations were investigated. In particular, high correlations have been obtained between the velocity dispersions σ_U , σ_V , σ_W , and σ_T and the age of the star, which clearly show a smooth increase of the velocity dispersions in the U, V, W components and total velocity T with time. From the calibration by Holmberg et al. (2009) these correlations can be approximately written as

$$\log \sigma = a \log t + b , \quad (4)$$

where the age t is in Gyr and the constants a , b are given in Table 2. This approximation is valid in the age interval $0 < t(\text{Gyr}) < 14$ with an estimated average age uncertainty of about 25%. Method 1 consists of assuming that the discrepancy in the rotation velocity $\Delta\theta$ is due to the evolved status of the CSPN, so that we should expect a correlation between $\Delta\theta$ and the velocity dispersion, as given by Eq. (4). Since in this method we are using the rotation velocity, we have considered two possibilities, according to which the velocity discrepancy $\Delta\theta$ can be associated with (i) the V component of the total velocity (σ_V), or (ii) the total velocity (σ_T). Moreover, since we are adopting two distance scales and two theoretical rotation curves, we have 8 different age distributions for Method 1, characterized by the timescales t_1 to t_8 , as explained in Table 3.

2.2. Method 2: The U , V , W velocity components

Method 2 is also a kinematic method, and in principle more accurate than Method 1, as discussed in more detail in Section 4. From the PN radial velocities and distances, we have estimated their proper motions both in right ascension and declination, μ_α and μ_δ . We have assumed that, in average, the tangential velocities are similar to the radial velocities, namely $V_t \simeq V_r$. In view of the large distances of the nebulae, this hypothesis in practice does

TABLE 3
PARAMETERS FOR METHOD 1.

Distance	Rotation Curve	Dispersion	Age
Maciel	PN	σ_V	t_1
Maciel	PN	σ_T	t_2
Maciel	Clemens	σ_V	t_3
Maciel	Clemens	σ_T	t_4
Stanghellini	PN	σ_V	t_5
Stanghellini	PN	σ_T	t_6
Stanghellini	Clemens	σ_V	t_7
Stanghellini	Clemens	σ_T	t_8

not introduce any major uncertainties in the results. Considering further the equatorial coordinates (α, δ) of the PN, we have used the equations by Boesgaard and Tripicco (1986) to derive the U , V , W velocity components of the nebulae, as well as the total velocity T and the velocity dispersions σ_U , σ_V , σ_W , and σ_T . According to these equations we derive the following parameters: $C = f(d)$, $X = f(C, \mu_\alpha, \mu_\delta, \alpha, \delta, V_r)$, $Y = f(C, \mu_\alpha, \mu_\delta, \alpha, \delta, V_r)$, and $Z = f(C, \mu_\delta, \delta, V_r)$, from which the velocities can be written as $U = f(X, Y, Z)$, $V = f(X, Y, Z)$, $W = f(X, Y, Z)$, and $T = f(X, Y, Z)$, so that the dispersions are given by

$$\sigma_i = \sqrt{(V_i - \bar{V}_i)^2} \quad (5)$$

where V_i stands for the velocities U, V, W, T . Then, we have again used the detailed correlations between the velocity dispersions and the ages as given by the Geneva-Copenhagen survey (Holmberg et al. 2009), adopting the same coefficients given in Table 2. We have used the same distance scales (Maciel 1984 and Stanghellini et al. 2008), so that we have again 8 different age distributions, corresponding to the timescales t_9 to t_{16} , as described in Table 4.

In practice, we have considered several additional cases, in order to better investigate the hypothesis of $V_i \simeq V_r$. Assuming that these velocities are of the same magnitude, but allowing for the possibility of different signs, we have as a result several possibilities for the proper motions μ_α and μ_δ , all of which are consistent with either $V_i \simeq V_r$ or $|V_i| \simeq |V_r|$. It turns out that these possibilities produce very similar age distributions, which will be discussed in Section 4. Therefore, we will present only the distributions of the ages t_9 to t_{16} , as defined in Table 4, for the cases where $\mu_\alpha \simeq \mu_\delta \simeq 0$.

An interesting alternative to overcome the lack of proper motion and tangential velocity measurements would be to apply the singular value decomposition (SVD) technique, as used by Branham (2010) to solve the inverse problem, that is, obtaining the space velocities from available proper motions. However, in view of the similarity of the results for different assumptions

TABLE 4
PARAMETERS FOR METHOD 2.

Distance	Dispersion	Age
Maciel	σ_U	t_9
Maciel	σ_V	t_{10}
Maciel	σ_W	t_{11}
Maciel	σ_T	t_{12}
Stanghellini	σ_U	t_{13}
Stanghellini	σ_V	t_{14}
Stanghellini	σ_W	t_{15}
Stanghellini	σ_T	t_{16}

regarding the tangential velocities, it is unlikely that this technique would produce very different results than presented here.

3. THE SAMPLES

As mentioned in the Introduction, we have considered two samples of Milky Way PN. In order to make comparisons with our previous work, we have first considered the same sample used by Maciel et al. (2003, 2005, 2006), which we will call Sample 1. This sample contains 234 well-observed nebulae located in the solar neighbourhood and in the disk, for which all data were obtained with the highest accuracy. Their Galactocentric distances are in the range $4 < R(\text{kpc}) < 14$, and most (69%) are located in the solar neighbourhood, with distances $d < 3 \text{ kpc}$.

The second sample considered in this work, called Sample 2, includes all the nebulae for which accurate radial velocities are available in the catalogue by Durand et al. (1998), comprising 867 objects. This is a more complete sample, so that it is expected that the derived results can be extended to the observed population of PN in the Galaxy. In both samples, the number of nebulae used depends on the availability of the statistical distances. The actual number of objects from the Maciel (1984) and Stanghellini et al. (2008) distance scales are 195 and 170 for Sample 1 and 493 and 403 for Sample 2, respectively. We have then applied the approximation given by Eq. (4) for both samples, with the coefficients shown in Table 2, considering only the objects for which ages in the interval $0 < t(\text{Gyr}) < 14$ could be obtained.

4. RESULTS AND DISCUSSION

The main results for the age distribution of the CSPN are shown in Figures 1-4, where we have used the age parameter definitions given in Tables 3 and 4 for Methods 1 and 2, respectively. Figures 1 and 2 refer to Sample 1, while

TABLE 5
 FRACTION OF STARS AT THREE AGE INTERVALS.

	Δt (Gyr)	0 – 3	3 – 6	> 6
Method 1	t_1	0.57	0.13	0.30
	t_2	0.62	0.18	0.20
	t_3	0.57	0.19	0.24
	t_4	0.67	0.18	0.16
	t_5	0.51	0.13	0.36
	t_6	0.71	0.17	0.12
	t_7	0.61	0.15	0.24
	t_8	0.71	0.11	0.18
Method 2	t_9	0.76	0.12	0.12
	t_{10}	0.79	0.10	0.11
	t_{11}	0.92	0.04	0.04
	t_{12}	0.77	0.18	0.05
	t_{13}	0.78	0.10	0.12
	t_{14}	0.78	0.11	0.11
	t_{15}	0.93	0.03	0.04
	t_{16}	0.76	0.18	0.06

figures 3 and 4 refer to Sample 2. It can be seen that the age distributions obtained by both methods are similar, in the sense that most objects have ages under 5 Gyr, with a strong peak at ages typically between 1 and 3 Gyr. The histograms of Figures 3-4 are summarized in Table 5, where the fraction of stars obtained by Method 1 (ages t_1 to t_8) and Method 2 (ages t_9 to t_{16}) are shown for three age bins, namely 0 – 3 Gyr, 3 – 6 Gyr, and $t > 6$ Gyr.

The similarity of the results of both methods is remarkable, especially considering that Method 2 is probably more accurate than Method 1. Method 2 consists of straightforward calculations of the velocities and velocity dispersions followed by an application of relatively accurate correlations involving the kinematics and ages of the objects considered. On the other hand, Method 1 is based on the assumption that the differences between the observed and predicted rotation velocities are essentially due to age effects. However, other processes may be important, such as deviations from the circular rotation, which is particularly important for nearby objects. According to Table 5, in all cases the vast majority of CSPN have ages under 3 Gyr. For Method 1 the total fraction of objects with $t \leq 3$ Gyr is 50 – 70%, while for Method 2 this fraction is somewhat higher, 70 – 90%. It is unlikely that this is a result from biased samples, as the results for the larger Sample 2 are essentially the same as in the smaller Sample 1. It should be pointed out that the latter, albeit smaller, includes only well studied nebulae, for which all individual

parameters (distances, velocities, abundances) are better determined.

Also, there are no significant differences in the results using the different velocity components U , V , W , and T . For Method 1, the distributions using the V velocity component are essentially the same as those using the total velocity, for both distance scales and samples. For Method 2, the distributions are slightly more concentrated in the first few age bins for the W component, compared with the distributions for the U and V components and the total velocity, again for both distance scales and samples. Since the W component is more clearly associated with the disk heating, essentially caused by age effects, the corresponding distributions are probably more accurate.

Similar remarks can be made regarding the adopted values for the proper motions. As mentioned at the end of Section 2, the results shown here assume that $\mu_\alpha \simeq \mu_\delta \simeq 0$. Adopting nonzero values for these quantities ($\mu_\alpha \simeq \mu_\delta \neq 0$), either the V or W component distributions become slightly less concentrated at the first few age bins, but most objects still have ages under about 4 Gyr. Again, the application of the SVD technique could be useful to confirm these results.

The uncertainties in the distances of the Milky Way PN are difficult to estimate, but the procedure adopted here ensures that the obtained age distributions are not particularly affected by the individual distances of the objects in the samples. As mentioned in Section 2, we have adopted two very different statistical scales, and the derived age distributions are essentially the same in both cases. The individual distances may depend on the particular scale, but the results shown in Figures 1–4 and in Table 5 do not depend on the choice of the distance scale. This can be seen by comparing the results for the timescales $t_1 - t_4$ with those for $t_5 - t_8$, or the results for $t_9 - t_{12}$ with those for $t_{13} - t_{16}$.

The uncertainties in the radial velocities also do not seem to have an important effect on the age distributions. In the catalogue by Durand et al. (1998), most objects ($\sim 90\%$) have uncertainties smaller than 20 km/s, and many objects have much lower uncertainties. Concerning Method 1, from Maciel & Lago (2005), the average rms deviation in the rotation velocity is about 50 km/s for PN, which can be compared with the values of about 20 km/s for HII regions (see also Clemens 1985 and Maciel & Dutra 1992).

Probably the main uncertainty of the age distributions is due to the calibration between the stellar ages and the velocity dispersions, given by Eq. (4), which affects both Method 1 and 2. From the Geneva-Copenhagen Survey, this relation has a dispersion of about 20 km/s in average, which corresponds roughly to an age uncertainty of about 25%, amounting to less than 1.2 Gyr for the objects of Figures 1–4. Therefore, the uncertainties of the present method are comparable and probably smaller than in the case of the methods based on age-metallicity relations considered by Maciel et al. (2010).

The results for Sample 2 are not essentially different from those of Sample 1, so that a direct comparison can be made with the results by Maciel et al. (2010). The results of both investigations are similar, even though the present

methods are completely independent of the metallicity-based methods used by Maciel et al. (2010). The main difference is that the kinematic methods used in the present investigation suggest somewhat lower ages for the CSPN in our samples. In this respect, these results fit nicely to the probability distribution for the progenitors of the CSPN according to Maciel et al. (2010, cf. figure 7, dashed line). In this case the well known relation between the main sequence mass and the stellar ages by Bahcall & Piran (1983) was adopted, taking $t = 10$ Gyr for $1M_{\odot}$ stars on the main sequence. Taking into account the uncertainties of the methods, which are typically in the range 1 – 2 Gyr, this case was considered as the most realistic, so that it is reassuring that the kinematic methods produce similar results.

Acknowledgements. We thank Dr. R. Branham, Jr., for some interesting comments on an earlier version of this paper. This work was partly supported by FAPESP and CNPq.

REFERENCES

- Bahcall, J. N., Piran, T. 1983, ApJ, 267, L77
 Boesgaard, A. M., Tripicco, M. J. 1986, ApJ, 303, 724
 Branham, R. L. Jr, 2010, MNRAS, 409, 1269
 Cahn, J. H., Kaler, J. B., & Stanghellini, L. 1992, A&AS, 94, 399
 Clemens, D. C. 1985, ApJ, 295, 422
 Daub, C. T. 1982, ApJ, 260, 612
 Durand, S., Acker, A., & Zijlstra, A., 1998, A&S, 132, 13
 Holmberg, J., Nordström, B., Andersen, J. 2007, A&A, 475, 519
 Holmberg, J., Nordström, B., Andersen, J. 2009, A&A, 501, 941
 Maciel, W. J. 1984, A&AS, 55, 253
 Maciel, W. J., Costa, R. D. D., & Idiart, T. E. P. 2010, A&A, 512, A19
 Maciel, W. J., Costa, R. D. D., & Uchida, M. M. M. 2003, A&A, 397, 667
 Maciel, W. J., Dutra, C. M. 1992, A&A, 262, 271
 Maciel, W. J., Lago, L. G. 2005, Rev. Mex. A&A, 41, 383
 Maciel, W. J., Lago, L. G., & Costa, R. D. D. 2005, A&A, 433, 127
 Maciel, W. J., Lago, L. G., & Costa, R. D. D. 2006, A&A, 453, 587
 Nordström, B., Mayor, M., Andersen, J. et al. 2004, A&A, 418, 989
 Perryman, M. 2009, Astronomical Applications of Astrometry: Ten Years of Exploitation of the Hipparcos Satellite Data, CUP
 Reid, M. 2010, Dynamics from the Galactic Center to the Milky Way Halo, 6th. Harvard-Smithsonian Conference on Theoretical Astrophysics, Online Publication, <http://www.cfa.harvard.edu/events/2010/dyn>
 Stanghellini, L., Shaw, R. A., & Villaver, E. 2008, ApJ, 689, 194

W. J. Maciel, T. S. Rodrigues and R. D. D. Costa: Instituto de Astronomia, Geofísica e Ciências Atmosféricas, Universidade de São Paulo - Rua do Matão 1226, CEP 05508-090, São Paulo SP, Brazil (maciel@astro.iag.usp.br, tsrodrigues@usp.br, roberto@astro.iag.usp.br.)

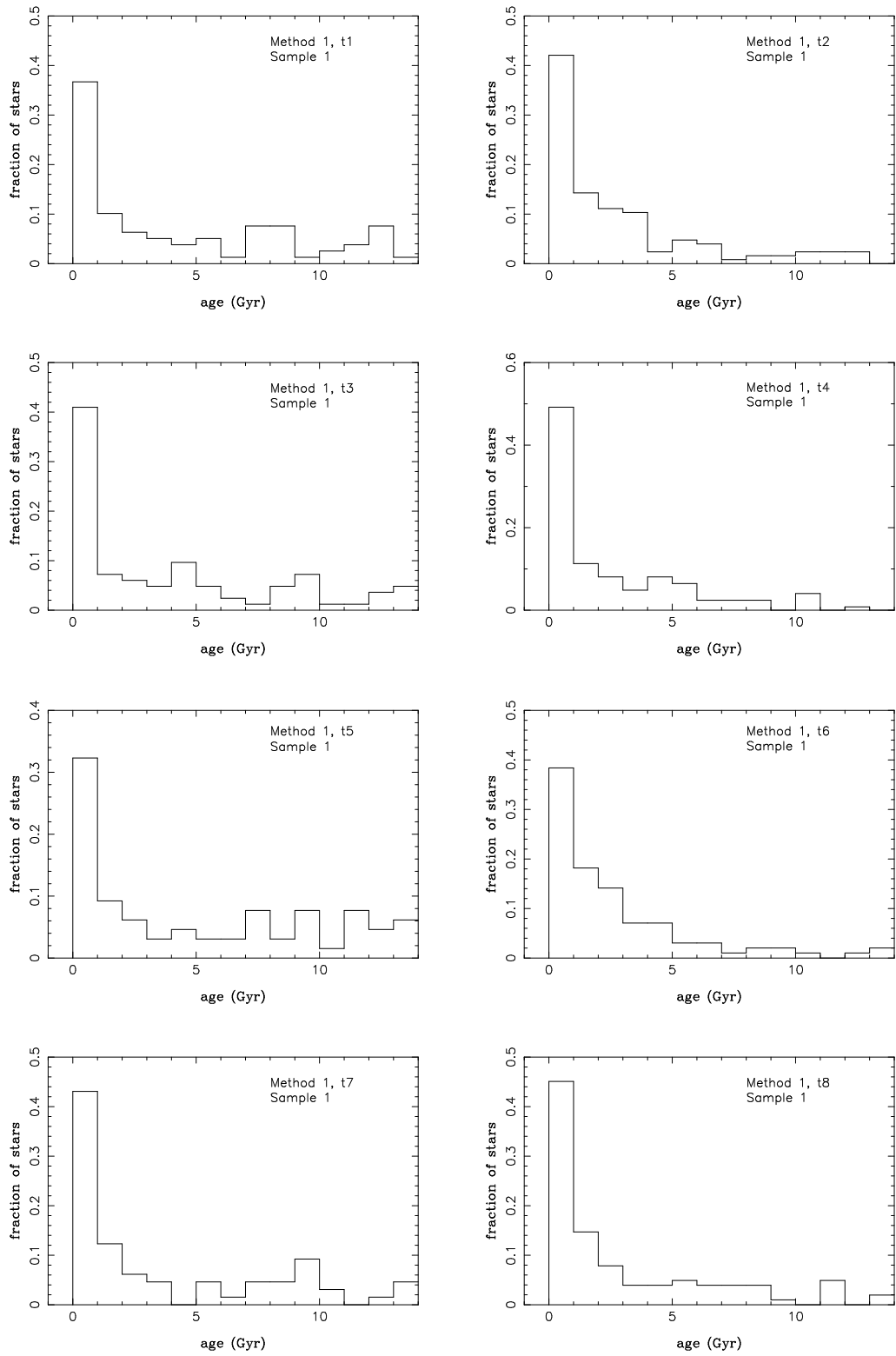


Fig. 1. Age distribution of CSPN, Method 1, Sample 1.

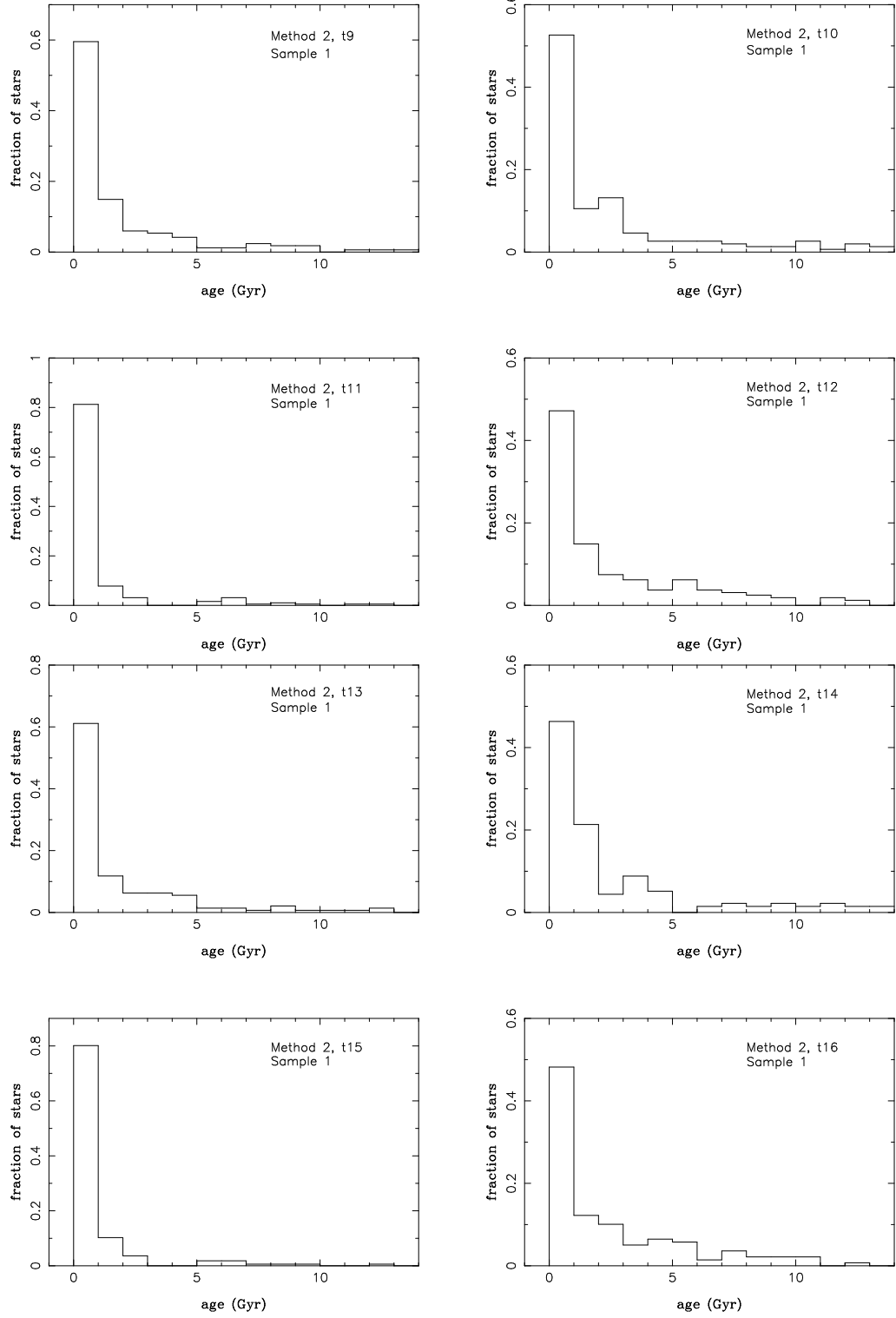


Fig. 2. Age distribution of CSPN, Method 2, Sample 1.

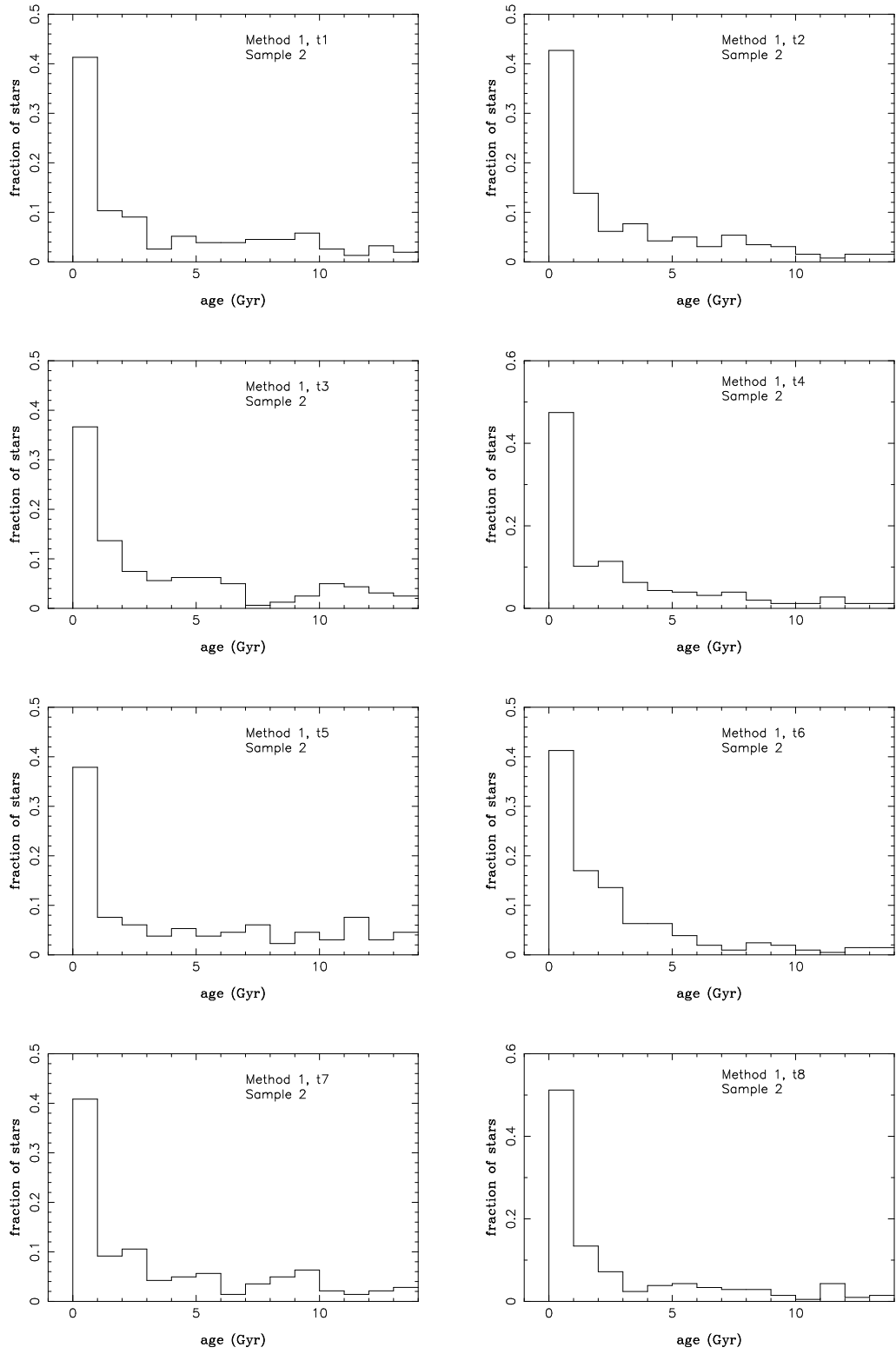


Fig. 3. Age distribution of CSPN, Method 1, Sample 2.

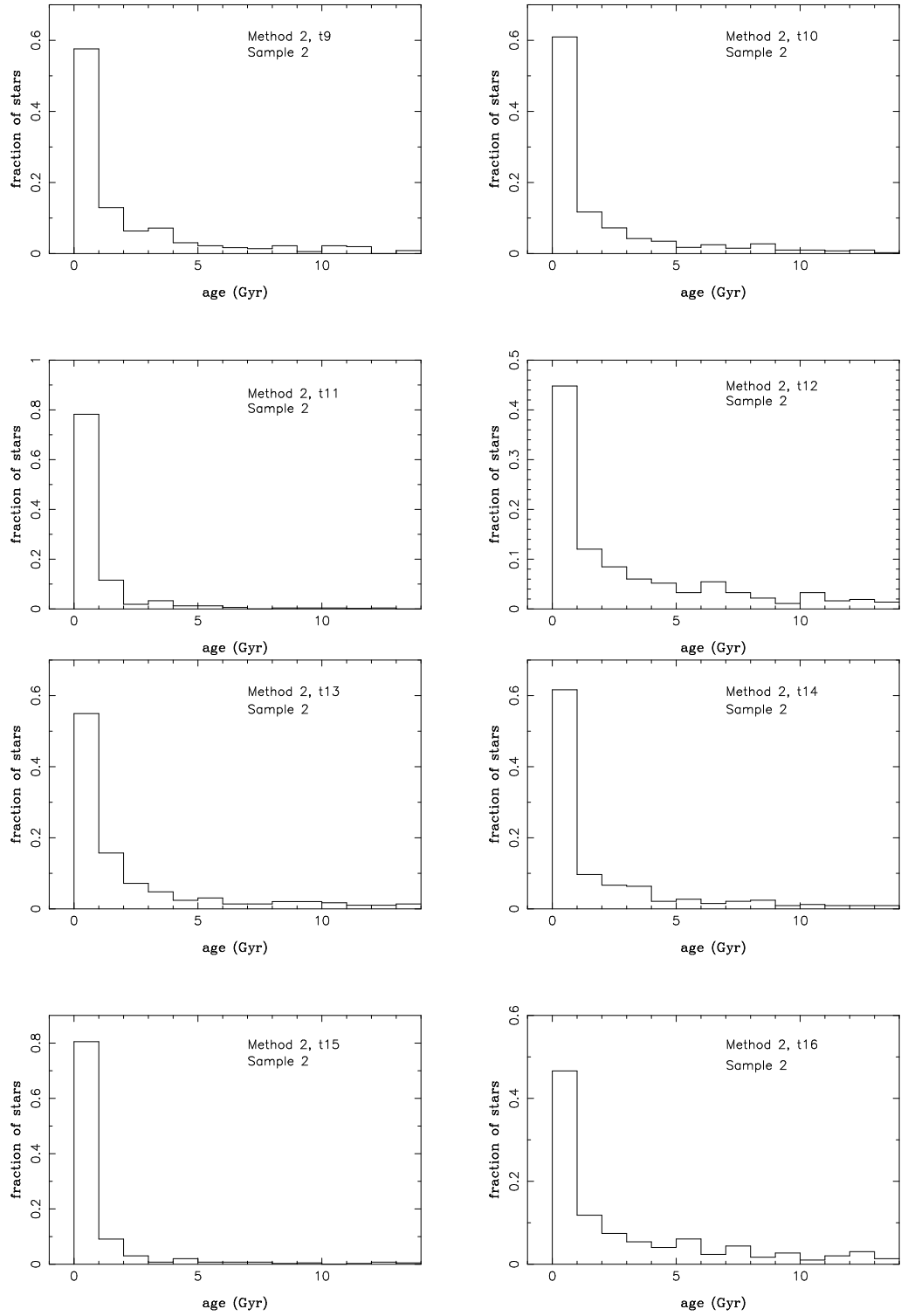


Fig. 4. Age distribution of CSPN, Method 2, Sample 2.